Effect of High-Pressure Ammonia Treatment on the Activity of Ge_3N_4 Photocatalyst for Overall Water Splitting

Yungi Lee,[†] Tomoaki Watanabe,[‡] Tsuyoshi Takata,[†] Michikazu Hara,[||] Masahiro Yoshimura,[‡] and Kazunari Domen*[,†,§]

Department of Chemical System Engineering, The University of Tokyo, 7-3-1 Hongo, Bunkyo-ku, Tokyo, 113-8656, Japan, Chemical Resources Laboratory, Tokyo Institute of Technology, 4259 Nagatsuta, Midori-ku, Yokohama, 226-8503, Japan, Materials and Structures Laboratory, Tokyo Institute of Technology, 4259 Nagatsuta, Midori-ku, Yokohama, 226-8503, Japan, and Solution-Oriented Research for Science and Technology (SORST), Japan Science and Technology Co. (JST), 2-1-13 Higashiueno, Taito-ku, Tokyo 110-0015, Japan

Received: May 18, 2006; In Final Form: July 20, 2006

The photocatalytic activity of β-Ge_3N_4 powder for overall water splitting is successfully enhanced by ammonia treatment at 823 K for 5−24 h at ammonia pressures of 20 MPa or greater. The surface and bulk nitrogen content in the treated samples varies according to the treatment temperature and treatment time, related to the stability of β-Ge_3N_4 powder under pressurized ammonia. The change in nitrogen content resulted in a change in the photocatalytic activity for overall water splitting. A β-Ge_3N_4 powder treated at 823 K for 5 h under ammonia at 20 MPa exhibited a photocatalytic activity 4 times higher than that of the as-synthesized powder, attributable to a decrease in the density of anion defects in the bulk and surface.

Introduction

Photocatalysts for overall water splitting have been studied extensively for the purpose of energy conversion from solar radiation to hydrogen as an energy carrier. Only a few transition-metal oxides containing Ti^{4+}, Zr^{4+}, Nb^{5+}, or Ta^{5+} with d^0 electronic configuration[1−6] and typical metal oxides containing Ga^{3+}, In^{3+}, Ge^{4+}, Sn^{4+}, or Sb^{5+} with d^{10} electronic configuration[7−9] have been found to achieve overall water splitting into H_2 and O_2. The valence bands of these metal oxides are mainly composed of O 2p orbitals, while the conduction bands are composed of empty metal d orbitals with d^0 electronic configuration or metal sp hybrid orbitals with d^{10} electronic configuration. The deep positive potential of the O 2p orbitals constituting the top of the valence band results in band gaps greater than 3.0 eV in these metal oxides, allowing only light in the ultraviolet (UV) region to stimulate the overall water splitting reaction. Thus, despite the success of these catalysts for overall water splitting, it remains a serious drawback that these metal oxides can only utilize 2−3% of the solar radiation reaching the earth's surface. Substantial effort has therefore been made to sensitize photocatalysts for visible-light activity. Although various nonoxide materials, such as CdS[10] and CdSe,[11] have been examined as potential visible-light-activated photocatalysts, little success has been achieved, primarily because of the instability of such photocatalysts.

Some of the present authors have recently reported (oxy)-nitrides or (oxy)sulfide including early transition metals with d^0 electronic configuration, such as Ta_3N_5,[12] TaON,[13] and $LaTiO_2N$[14] or $Sm_2Ti_2S_2O_5$,[15] or typical metals with d^{10} electronic configuration, such as $(Ga_{1-x}Zn_x)(N_{1-x}O_x)$[16] and Ge_3N_4,[17] as potential candidates for overall water splitting under visible-light irradiation. These photocatalysts with d^0 electronic configuration have yet to achieve the decomposition of water into H_2 and O_2, probably because of the presence of significant densities of defects in the bulk and surfaces of the materials. In contrast, the typical metal (oxy)nitride photocatalysts with d^{10} electronic configuration have been used successfully to decompose water under UV or visible-light irradiation, although the quantum efficiency remains low because of high-defect densities caused by the reducing atmosphere required in current preparation procedures.[17] The activity of these (oxy)nitride photocatalysts is thus expected to be improved by refining the preparation method or by modifying the as-synthesized materials.

High-pressure ammonia treatment is one method that has been examined as a means of reducing the number of defects and impurities in as-prepared (oxy)nitride. Pressurized ammonia is highly unstable and reactive at high temperature, similar to H_2O in hydrothermal synthesis. Yoshimura et al. reported that the nitridation of a mixture of ammonium chloride, NH_4Cl, and zirconium powder under pressurized ammonia yields ZrN at 873 K, which is a quite low synthesis temperature compared to that for conventional synthesis.[18] Majima et al. have found that iron nitride prepared from mechanical alloying contains more nitrogen when synthesized under higher NH_3 pressure.[19] It has long been known that certain metal nitrides are good catalysts for ammonia-based synthesis.[20−23] Segal et al. reported that in the case of uranium nitride, the active catalyst is the nonstoichiometric uranium sesquinitride phase, which has a wide range of nitrogen composition, making it possible to vary the nitrogen content of the catalyst during the reaction through adjustment of the temperature and nitrogen partial pressure.[22] It is thus

* To whom correspondence should be addressed. Address: Department of Chemical System Engineering, The University of Tokyo, 7-3-1 Hongo, Bunkyo-ku, Tokyo, 113-8656, Japan; phone: +81-3-5841-1148; fax: +81-3-5841-8838; e-mail: domen@chemsys.t.u-tokyo.ac.jp.

[†] Department of Chemical System Engineering, The University of Tokyo.

[‡] Materials and Structures Laboratory, Tokyo Institute of Technology.

[||] Chemical Resources Laboratory, Tokyo Institute of Technology.

[§] Solution-Oriented Research for Science and Technology (SORST), Japan Science and Technology Co. (JST).

10.1021/jp063068v CCC: $33.50
Published on Web 08/17/2006

expected that nitride photocatalysts may be suitably modified by high-pressure ammonia treatment.

In this study, high-pressure ammonia treatment is applied to as-synthesized β-Ge_3N_4 powder under various conditions, and the characteristics and photocatalytic activity of the treated β-Ge_3N_4 powder are investigated.

Experimental Section

Preparation and High-Pressure Treatment. β-Ge_3N_4 powder was prepared by reaction of GeO_2 (>99.99%, High Purity Chemical) with ammonia (>99.999%, Fujiox) for 10 h under atmospheric pressure, at a flow rate of 100 mL·min^{-1} and a temperature of 1173 K. This as-prepared β-Ge_3N_4 powder was then subjected to high-pressure treatment as follows. A 0.6-g sample of the powder was placed in an unsealed gold tube and was evacuated in a test tube-type pressure reactor. The reactor was then heated to the appropriate treatment temperature varied from 723 to 973 K at ammonia pressure of 0.1 MPa to 50 MPa for 5−72 h. After high-pressure treatment, the samples were taken from the gold tube in air and were characterized.

Characterization. The structures were characterized by X-ray diffractometry (XRD; RINT 2100, Rigaku) using Cu K_α radiation at 40 kV and 40 mA. The XRD patterns were collected at 2θ angles of 10−70° at a scan rate of 4° min^{-1}. Raman spectroscopy (NRS-2100, Jasco) was also employed to verify the phases of β-Ge_3N_4 powder before and after high-pressure treatment. The Raman spectra were obtained using the 514.5 or 488 nm line of an Ar-ion laser. UV−visible diffuse reflectance spectrometry (DRS; V-560, Jasco) was performed in reference to $BaSO_4$ powder. The contents of nitrogen in the samples were analyzed by elemental analysis (CHNS-932, LECO). Thermogravimetric and differential thermal analysis (TG-DTA; DTG-50H, Shimadzu) was performed to observe the decomposition temperature of the powders using ca. 20 mg of sample by heating at 10 K·min^{-1} to 1373 K under air flow at 50 mL·min^{-1}. The surface morphologies and average particle sizes of products were observed by field-emission scanning electron microscopy (SEM; S-4700, Hitachi). The surface areas were determined by Brunauer, Emmett, and Teller (BET) measurements (SA3100, Coulter). The surfaces of the β-Ge_3N_4 powder were examined by X-ray photoelectron spectroscopy (XPS; ESCA 3200, Shimadzu). All binding energies were corrected using the binding energy of Au $4f_{7/2}$ (83.8 eV). Photoluminescence measurements are conducted using a spectrofluorometer (FP-660, Jasco) with 200 W Xe lamp at 77 K.

Photocatalytic Reactions. Photocatalytic reactions were carried out in a closed gas circulation system. RuO_2 (1 wt %) was loaded as a cocatalyst by the impregnation method using triruthenium dodecacarbonyl ($Ru_3(CO)_{12}$, 99%, Aldrich) dissolved in tetrahydrofuran (99.5%, Nacalai Tesque) and subsequent calcination at 673 K for 3 h in air. This procedure loaded RuO_2 onto the surface of the β-Ge_3N_4 photocatalyst. A 0.5-g sample of the treated β-Ge_3N_4 powder loaded with RuO_2 was dispersed in distilled water using a magnetic stirrer in an inner-irradiation quartz reaction cell. Before the reaction, the system was degassed and then was filled with a small amount of Ar gas (30 Torr). A 450-W high-pressure mercury lamp (UM-452, Ushio) was employed as a light source.

Results and Discussion

Effect of Ammonia Pressure on Photocatalytic Activity. High-pressure ammonia treatment was carried out under 20−50 MPa of ammonia at 823 K for 5 h. For comparison, another sample of as-prepared β-Ge_3N_4 powder was also treated at 823 K for 5 h under atmospheric ammonia. The positions and intensities of XRD peaks remained unchanged upon treatment for all samples, with all peaks assignable to a single phase of β-Ge_3N_4. Additional phases such as GeO_2, Ge, or α-Ge_3N_4 were not observed. Figure 1 shows the photocatalytic activities of the treated samples for overall water splitting. The samples treated with pressurized ammonia exhibited greater photocatalytic activity than the as-synthesized β-Ge_3N_4 powder, while the sample treated at 0.1 MPa of ammonia showed only a slight increase in photocatalytic activity.

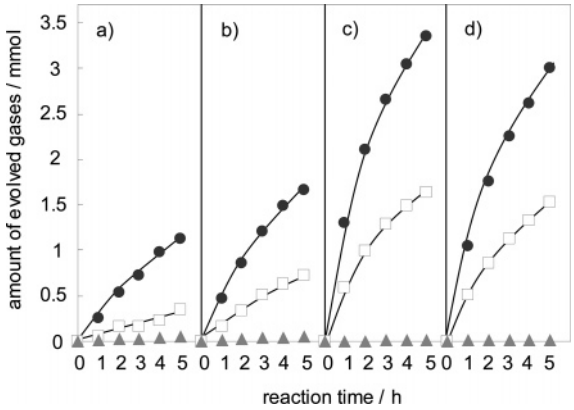

Figure 1. Time courses of evolved gases for β-Ge_3N_4 powders loaded with RuO_2 (1 wt %) as a cocatalyst. (a) As-synthesized powder. (b−d) Samples treated at 823 K for 5 h with (b) 0.1 MPa, (c) 20 MPa, and (d) 50 MPa of NH_3. Circles denote H_2 evolution, squares denote O_2 evolution, and triangles denote N_2 production.

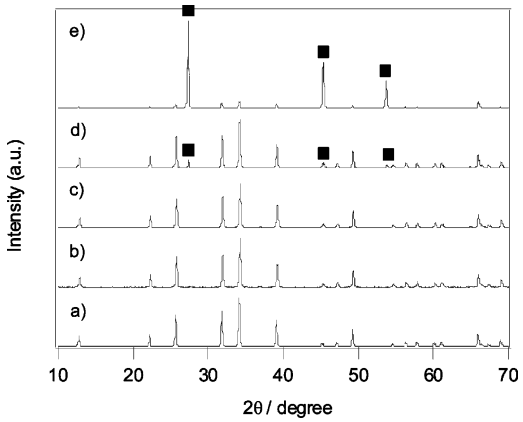

Figure 2. XRD patterns for β-Ge_3N_4 powders. (a) As-synthesized powder. (b−e) Samples treated for 5 h with 20 MPa of NH_3 at (b) 723 K, (c) 823 K, (d) 923 K, and (e) 973 K. Solid squares denote peaks due to Ge.

Chemical analyses revealed that the nitrogen content of the β-Ge_3N_4 powder was decreased from 20.47 wt % to 20.22 wt % after the treatment at 0.1 MPa, while it remained at the calculated value of 20.47 wt % for treatment at high pressure, indicating that high pressure is necessary to modify the sample without release of nitrogen from the samples. These results demonstrate that pressurized ammonia treatment is effective for enhancing the photocatalytic activity of β-Ge_3N_4 powder for overall water splitting.

Effect of Treatment Temperature on Photocatalytic Activity. Figure 2 shows XRD patterns of the samples before and after high-pressure ammonia treatment at various temperatures for 5 h at 20 MPa. Samples treated at less than 923 K exhibited only peaks assignable to a single phase of β-Ge_3N_4. With treatment at temperatures of 923 K or higher, however, peaks

TABLE 1: Nitrogen Content in β-Ge_3N_4 Powders, As-Synthesized and Treated for 5 h with 20 MPa of NH_3 at Various Treatment Temperatures

			after high-pressure ammonia treatment[a]			
	calculated	as-synthesized	723 K	823 K	923 K	973 K
nitrogen content/wt %	20.47	20.47	19.80	20.47	19.29	3.52

[a] Treatment for 5 h under 20 MPa NH_3.

due to germanium began to appear. At 973 K, almost all peaks could be attributed to germanium, indicating that the β-Ge_3N_4 phases had been transformed to germanium by treatment at this temperature.

The nitrogen content before and after high-pressure ammonia treatment (see Table 1) is in good agreement with the XRD patterns of the treated samples. The as-synthesized β-Ge_3N_4 powder and samples treated at 823 K have a nitrogen content of 20.47 wt %, which coincides well with the value calculated from the theoretical composition of germanium nitride (Ge_3N_4) and the XRD results showing a single phase of β-Ge_3N_4 to be present. The nitrogen content decreased to 19.80 wt % upon treatment at 723 K at which no change in the XRD pattern was observed, while it decreased to 19.29 wt % upon treatment at 923 K at which a small amount of germanium was detected in the XRD pattern, and then it dropped abruptly to 3.52 wt % in the sample treated at 973 K which exhibited peaks assignable to Ge phase with low intensity of β-Ge_3N_4 phase. The TG-DTA measurements indicate that nitrogen in the β-Ge_3N_4 powder is released at temperatures higher than 973 K in air. The decomposition temperature of β-Ge_3N_4 powder therefore appears to be 973 K under this condition. However, during high-pressure ammonia treatment, nitrogen in the β-Ge_3N_4 powder began to be released at 723 K, a temperature much lower than the decomposition temperature in air. In analysis of the stability of β-Ge_3N_4 powder under various conditions,[24] Johnson showed that β-Ge_3N_4, while highly stable toward oxidizing reagents, is readily reduced to metallic germanium under a hydrogen stream at temperatures as low as 873 K, with reduction occurring very rapidly at 973 K. High-pressure treatment with ammonia, also a reducing gas, similarly results in the facile reduction of β-Ge_3N_4 to Ge at relatively low temperature.

Figure 3 shows the Raman spectra for β-Ge_3N_4 powder before and after high-pressure ammonia treatment at 823 K for 5 h at 20 MPa. Deb et al. reported that factor group analysis predicts 11 Raman active modes for β-Ge_3N_4, which was subsequently confirmed by experiments.[25] The Raman spectra for the as-synthesized β-Ge_3N_4 powder show these 11 active modes without other spectra because of Ge or GeO_2 phases. Leinenweber et al. reported that the phase transition from β-Ge_3N_4 to the high-pressure γ-Ge_3N_4 structure occurs at temperatures above 1273 K and under nitrogen at pressures greater than 12 GPa.[26] Dong et al. reported the structural change of β-Ge_3N_4 to γ-Ge_3N_4 at high pressure on the basis of comparison of theoretical analysis with X-ray and Raman scattering measurements.[27] Calculations showed that the near-planar Ge_3N units within the β-Ge_3N_4 structure pucker above a pressure of 20 GPa, lowering the symmetry from hexagonal $P6_3/m$ to hexagonal $P6$. Upon further application of pressure, the space group changes to $P3$. These distorted phases are derivatives of the β phase but have the $P6$ or $P3$ space group and only exist at high pressure if the temperature is insufficient to allow the $\beta \rightarrow \gamma$ transformation. In this study, after ammonia treatment at 823 K with 20 MPa, no spectral features other than those attributable to the 11 active modes of β-Ge_3N_4 powder were detected in the Raman

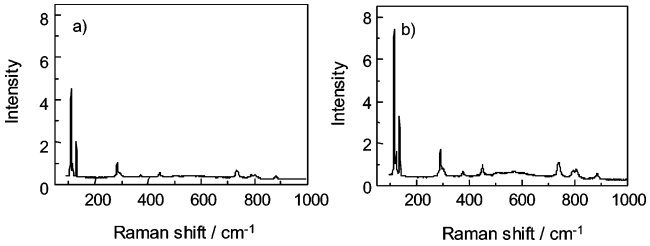

Figure 3. Raman spectra for β-Ge_3N_4 powders. (a) As-synthesized powder. (b) Sample treated for 5 h with 20 MPa of NH_3 at 823 K.

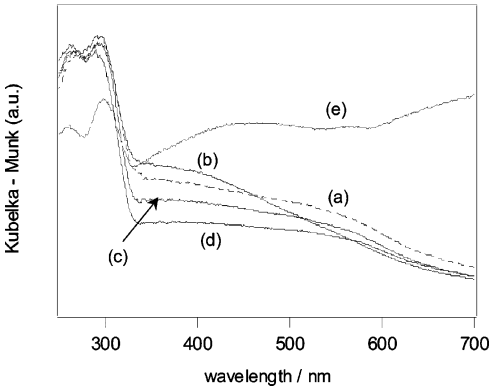

Figure 4. UV-visible DR spectra for β-Ge_3N_4 powders. (a) As-synthesized powder. (b−e) Samples treated for 5 h with 20 MPa of NH_3 at (b) 723 K, (c) 823 K, (d) 923 K, and (e) 973 K.

spectra, indicating that no reduction to Ge, no phase transition to the high-pressure γ-Ge_3N_4 structure, and no symmetry reduction occurred during treatment.

The phase change from β-Ge_3N_4 to Ge upon high-pressure ammonia treatment also affected the UV−visible DR spectra of the treated samples, as shown in Figure 4. The as-synthesized β-Ge_3N_4 powder exhibits two absorption bands: one strong absorption in the UV region below 340 nm and a broad absorption extending into the visible region. The absorption in the UV region is attributed to the band gap transition, which can be confirmed by coincidence with the edges of the excitation and emission bands in the photoluminescence spectra.[17] The absorption at longer wavelengths of up to 700−800 nm is regarded to be due to impurities and defect sites, such as reduced Ge species (Ge^0, Ge^{2+}). After high-pressure ammonia treatment at 723 K, the absorption in the visible-light region increased slightly, indicating the increase of nitrogen defects at this treatment temperature according to the decrease of nitrogen content from 20.47 wt % to 19.80 wt %. The absorption in the visible region decreased with increasing treatment temperature above 823 K to 923 K but rose substantially for the sample treated at 973 K, attributable to the presence of the Ge phase, which has high absorption in this region. Decrease of absorption in the visible region of the treated sample at 823 K without any change of nitrogen content showed that treatment under high-pressure ammonia at this treatment temperature region was effective for reducing the concentration of impurities and defects produced in the β-Ge_3N_4 powder during conventional preparation under a reductive atmosphere for nitridation. Although a change in absorption in the visible-light region was observed, the absorption edge in the UV region remained unchanged at 340 nm regardless of the treatment temperature.

The surface morphologies of the samples are presented in Figure 5. The morphology and average particle size of the samples treated below 923 K remained unchanged compared to the as-synthesized β-Ge_3N_4 powder, with an average particle

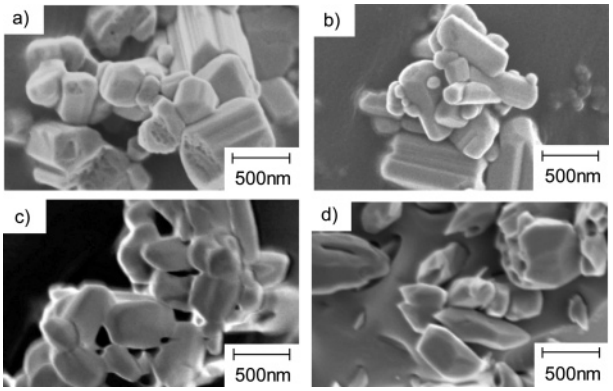

Figure 5. SEM images of β-Ge_3N_4 powders. (a) As-synthesized powder. (b−d) Samples treated for 5 h with 20 MPa of NH_3 at (b) 823 K, (c) 923 K, and (d) 973 K.

size of ca. 300 nm. As the treatment temperature increased from 923 to 973 K, however, grains began to aggregate and the boundaries between grains became increasingly unclear because of growth of the Ge phase.

Narrow-scan XPS spectra showing the Ge3d, N1s, and O1s peaks for the surfaces of the as-synthesized and ammonia-treated β-Ge_3N_4 powders are shown in Figure 6 for various treatment temperatures. The Ge3d peak for the as-synthesized powder was observed at 31.1 eV and was shifted slightly to higher binding energies of 31.7 and 31.5 eV upon treatment at 823 and 923 K, respectively, indicating that the states of Ge in the treated samples were changed to a more higher oxidation state. This result suggests that the high-pressure ammonia treatment is quite effective to decrease the reduced Ge species (Ge^0, Ge^{2+}) contained in the as-synthesized β-Ge_3N_4 powder. Despite the slight shift of Ge3d peak after high-pressure treatment, the Ge3d peak positions in all samples were located between that for metallic Ge (29.0 eV[28]) and that for GeO_2 (32.1 eV[29]). Although the metallic Ge phase was detected in the XRD pattern, no peak splitting in Ge3d peak was observed in the sample treated at 923 K. The N1s peaks in the as-synthesized sample and in the samples treated at 823 and 923 K were located at 397.1, 397.8, and 397.5 eV, respectively, in good agreement with the literature data for the N1s peak in Ge_3N_4 powder.[30] The chemical shift of the N1s peak of the sample treated at 823 K was probably due to the higher surficial nitrogen content, leading to the change of chemical states between N and Ge after high-pressure ammonia treatment. Ingo et al. reported that the N1s peak was shifted to higher binding energy as the nitrogen content in SiN_x was increased. The variations of peak position for nitrogen were explained in terms of a single bonding configuration with three silicon surrounding atoms.[31] The O1s peaks were observed at 530.6−530.8 eV and thus represent lattice oxygen in the β-Ge_3N_4 powder. From the atomic ratio of Ge, calculated from the areas of the XPS spectra (Table 2), the surface nitrogen concentration of the as-synthesized powder is 1.30, lower than the calculated value of 1.33 for Ge_3N_4 powder. High-pressure treatment at 823 K increased the nitrogen concentration on the sample surface from 1.30 to 1.32, whereas treatment at 923 K reduced the nitrogen concentration to 1.00. In contrast, the lattice oxygen concentration decreased upon treatment at 823 K, yet increased slightly upon treatment at 923 K. The increase in lattice oxygen in the sample treated at 923 K is probably because of impurities in the ammonia gas. On the basis of the report by Bauer that long reaction times are necessary for full equilibrium to be reached in the uranium−nitrogen system at 973 K,[32] it is considered that the reaction between β-Ge_3N_4 powder and pressurized ammonia would not have reached equilibrium in the 5 h of treatment employed in this study. Segal et al. reported that further nitridation of U_2N_3 is achieved by treatment at higher temperature, between 648 and 798 K.[33] In this temperature range, in which reaction between the reactant gases (nitrogen, hydrogen, and ammonia) and U_2N_3 did not reach equilibrium, a nitrogen species that becomes active at elevated temperature would have been present on the surface. Mallett et al. also found that the surface product produced in the direct nitridation of bulk uranium at 823 K and above is richer in nitrogen than regions in the bulk interior.[33] The present element analyses and XPS measurements have revealed that further nitridation was achieved in the bulk and on the surface by high-pressure ammonia treatment of the as-synthesized β-Ge_3N_4 powder for 5 h at 823 K, whereas the nitrogen content of samples treated at lower temperature (723 K) was lower. These results indicate that further nitridation of β-Ge_3N_4 powder is achieved at higher temperature (between 723 and 823 K), as observed for uranium nitride.[33] However, nitrogen in the bulk and on the surface was released from the as-synthesized β-Ge_3N_4 powder at higher treatment temperature (923 K) because of reduction of the β-Ge_3N_4 to Ge.

A plot of treatment temperature with respect to the rate of overall water splitting for samples treated for 5 h under 20 MPa is shown in Figure 7. The photocatalytic activity of products treated at 723 K was slightly lower than that of the as-synthesized β-Ge_3N_4 powder, attributable to the increase in nitrogen defects in the bulk (confirmed by elemental analysis). However, the rate of photocatalytic activity for overall water splitting increased with treatment temperature to a maximum at 823−923 K, above which the activity abruptly dropped. Treatment of β-Ge_3N_4 powder at 823 K effectively increased the photocatalytic activity by a factor of 4, yielding activities of 1.10 mmol·h^{-1} for H_2 evolution and 0.55 mmol·h^{-1} for O_2 evolution, in comparison with 0.26 mmol·h^{-1} and 0.05 mmol·h^{-1} for the as-synthesized powder. Our previous report reveals that the photocatalytic performance of RuO_2-loaded β-Ge_3N_4 was strongly dependent on the pH of aqueous solution, and a maximum activity was obtained at pH 0 with quantum efficiency of ca. 9.0%.[17] However, in the present experiments, all photocatalytic reactions were carried out in distilled water with pH 7 to eliminate any other effects than those of high-pressure ammonia treatments. The quantum efficiency of water splitting on β-Ge_3N_4 at around 300 nm is increased from ca. 2.0% to ca. 7.0% through the high-pressure ammonia treatment at 823 K.[35] These elevated activities can be attributed to a decrease in the density of impurities and defects in the β-Ge_3N_4 powder by treatment (confirmed by UV−visible DR spectra and XPS spectra). Slight decay of photocatalytic activities for all samples with increasing reaction time is attributed to the loosened interface connection between RuO_2 nanoparticles and Ge_3N_4, leading to inefficient electron transfer.[17] However, the sample treated at 973 K displays a marked drop in photocatalytic activity and did not produce H_2 and O_2 from water at a stoichiometric ratio. This low photocatalytic activity and lower production of O_2 is probably because of the presence of Ge in the treated sample, which does not exhibit photocatalytic activity for this reaction.

Effect of Treatment Time on Photocatalytic Activity. Figure 8 shows the XRD patterns of samples treated with ammonia at 823 K under 20 MPa for 5−72 h. The peaks exhibited by samples treated for 5−24 h can all be assigned to the single phase of β-Ge_3N_4, indicating the absence of impurities. However, Ge peaks with high intensity were detected for the

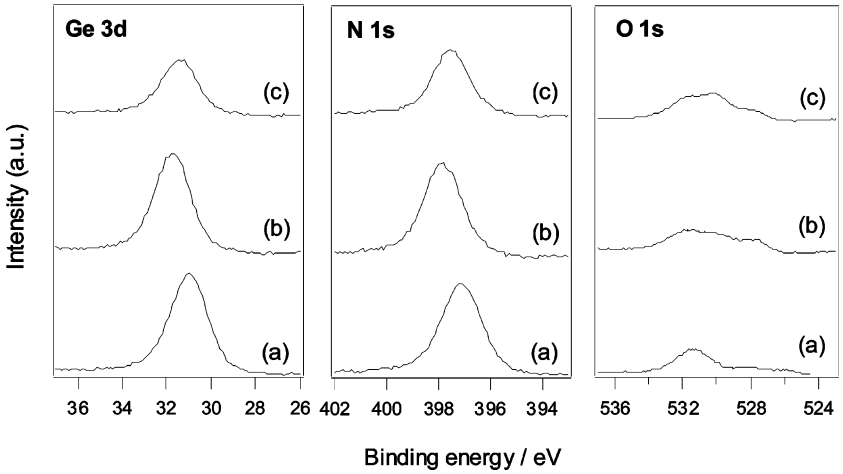

Figure 6. XPS spectra for β-Ge_3N_4 powders. (a) As-synthesized powder. (b−c) Samples treated for 5 h with 20 MPa of NH_3 at (b) 823 K and (c) 923 K.

TABLE 2: Atomic Ratio of N and O to Ge on β-Ge_3N_4 Surfaces

			after high-pressure ammonia treatment[a]	
	calculated	as-synthesized	823 K	923 K
N/Ge	1.33	1.30	1.32	1.00
O/Ge		0.15	0.07	0.54

[a] Treatment for 5 h under 20 MPa NH_3.

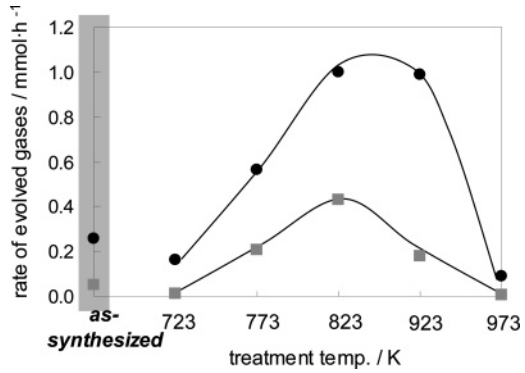

Figure 7. Rate of gas evolution over β-Ge_3N_4 powders, as-synthesized and treated for 5 h with 20 MPa of NH_3 at various treatment temperatures. Circles denote H_2 evolution and squares denote O_2 evolution.

sample treated for 72 h. Although the treatment temperature was lower than the decomposition temperature of β-Ge_3N_4 powder (973 K), this shows that nitrogen in β-Ge_3N_4 powder is readily released under reducing conditions during prolonged treatment.

As observed for samples treated under other treatment conditions, all treated samples exhibited weaker absorption in the visible region of the UV−vis DR spectra, as shown in Figure 9. The extent of absorption decrease due to treatment increased with treatment time to 24 h, indicating that nitridation advanced over this period, resulting in a gradual decrease in the density of defects and impurities in the β-Ge_3N_4 powder. After 72 h of treatment, however, the sample exhibited stronger absorption in the visible-light region, similar to the result for the sample treated at 973 K for 5 h, attributable to reduction of the as-synthesized β-Ge_3N_4 powder to Ge, which has strong absorption over a wide region of visible light.

Table 3 shows the nitrogen content in bulk and atomic ratio of N and O to Ge on the β-Ge_3N_4 surface. The atomic ratio of

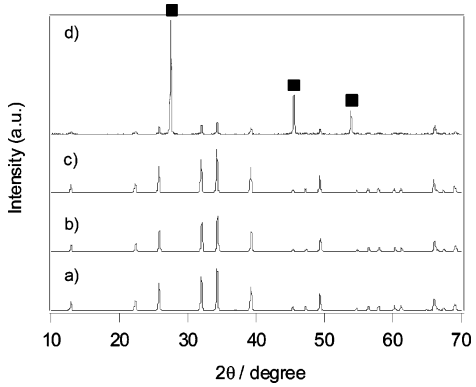

Figure 8. XRD patterns for β-Ge_3N_4 powders. (a) As-synthesized powder. (b−d) Samples treated at 823 K with 20 MPa of NH_3 for (b) 5 h, (c) 24 h, and (d) 72 h. Solid squares denote peaks due to Ge.

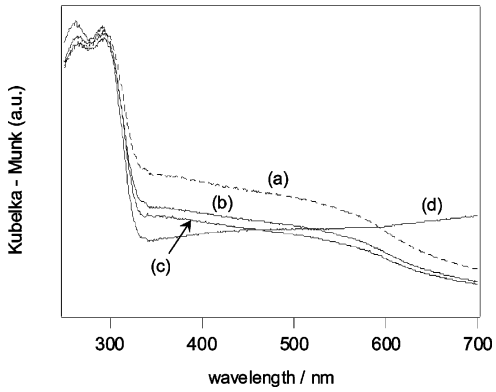

Figure 9. UV-visible DR spectra for β-Ge_3N_4 powders. (a) As-synthesized powder. (b−d) Samples treated at 823 K with 20 MPa of NH_3 for (b) 5 h, (c) 24 h, and (d) 72 h.

N to Ge on the β-Ge_3N_4 powder surface, calculated from the areas of the XPS spectra, reveals that the surface nitrogen concentration remained unchanged upon treatment for 5 h but then decreased upon further treatment up to 24 h. In contrast, nitrogen in the bulk was unchanged at 20.47 wt %, which is the theoretical nitrogen content in Ge_3N_4 during the nonequilibrium period in the first 24 h of treatment, and then decreased to 5.73 wt % upon treatment from 24 to 72 h. In this extended period, the reaction between the β-Ge_3N_4 powder and the gases in the reactor would have approached equilibrium. Although the nitrogen content in bulk was unchanged in the first 24 h, the surface nitrogen concentration decreased in this period,

TABLE 3: Nitrogen Content in Bulk and Atomic Ratio of N and O to Ge on the β-Ge_3N_4 Surface

				after high-pressure ammonia treatment[a]		
		calculated	as-synthesized	5 h	24 h	72 h
bulk[b]	nitrogen content/wt %	20.47	20.47	20.47	20.47	5.73
surface[c]	N/Ge	1.33	1.30	1.32	1.16	
	O/Ge		0.15	0.07	0.39	

[a] Treatment at 823 K under 20 MPa NH_3. [b] Elemental analyses. [c] XPS measurements.

indicating that nitrogen was released from the surface of the β-Ge_3N_4 powder.

Four main reactions are considered to occur between β-Ge_3N_4 powder and pressurized ammonia under the present treatment conditions as follows:

$$NH_3\,(g) \rightleftarrows N\,(a) + 3H\,(a) \quad (1)$$

$$2N\,(a) \rightleftarrows N_2\,(g) \quad (2)$$

$$2H\,(a) \rightleftarrows H_2\,(g) \quad (3)$$

$$N\,(a) \rightleftarrows N\,(bulk) \quad (4)$$

Treatment of β-Ge_3N_4 powder under 20 MPa ammonia proceeds to equilibrium in terms of both the gas and solid phases. During the treatments, as the pressure in the reaction tends to increase, mainly because of the forward reactions of 1−3, the total pressure was maintained at 20 MPa by releasing gas-phase molecules. After 5 h of treatment, the increase in total pressure had almost ceased, indicating that decomposition of gaseous ammonia was approaching equilibrium. Rough calculations using the equilibrium constant of reactions 1−4 at 823 K indicate that the equilibrium atmosphere should contain 0.88 MPa NH_3, 4.78 MPa N_2, and 14.34 MPa H_2. However, it is likely that the reaction between the gases and solid phase does not reach equilibrium in 5 h under the present conditions, such as the uranium−nitrogen system.[32] The reactions between the gases (nitrogen, hydrogen, and ammonia) and metal nitride have been reported by several researchers.[20−23] Aika et al.[23] reported that in ammonia synthesis (from nitrogen and hydrogen gas) over molybdenum nitride, the adsorbed nitrogen atoms via chemisoption process on catalyst surface were used for two reactions, that is, for ammonia synthesis (backward reaction of 1) or for exchange with the bulk nitrogen in catalyst (forward reaction of 4). The rate of exchange between the adsorbed and bulk nitrogen is 5 times smaller than that of ammonia synthesis. A similar tendency was reported for iron nitride by Logan et al.[20] Segal et al. found that adsorbed nitrogen tends to react with hydrogen (backward reaction of 1) for ammonia synthesis rather than penetrate into the bulk of uranium nitride (forward reaction of 4) at relatively low nitrogen pressures.[33] It is thus considered that the adsorbed nitrogen from pressurized ammonia (forward reaction of 1) or from bulk of catalyst (backward reaction of 4) is available for both exchange with the bulk nitrogen and release as gaseous nitrogen or ammonia produced through the reaction with hydrogen, the latter of which becomes more prominent as treatment time increases under low nitrogen partial pressure. The consumption of released nitrogen from the catalyst is in good agreement with the present experimental results showing a gradual reduction of the as-synthesized β-Ge_3N_4 powder to Ge phase with increasing treatment time.

Figure 10 shows the photoluminescence spectra at 77 K for samples treated for various periods. The onset of excitation (340 nm) coincides with the onset of UV−visible emission for all samples, indicating that the emission is due to the recombination of photogenerated electrons and holes. In the emission spectra for an excitation wavelength of 240 nm, the as-synthesized β-Ge_3N_4 powder exhibits an intense peak at ca. 410 nm, while the peak is shifted slightly to 430 nm in samples treated for 5−24 h. The intensity of emission increased with treatment time. The relationship between photoluminescence intensity and photocatalytic activity has been examined by many authors.[36,37] Anpo et al. reported that the change in intensity of the photoluminescence peak appears to parallel the change in yield of photocatalytic hydrogenation over titanium−silicon oxide catalysts with varying titanium-to-silicon ratios.[35] The low photoluminescence efficiency is considered to reflect an increase in the prevalence of nonradiative transition in photocatalysts, leading to a decrease in photocatalytic activity.

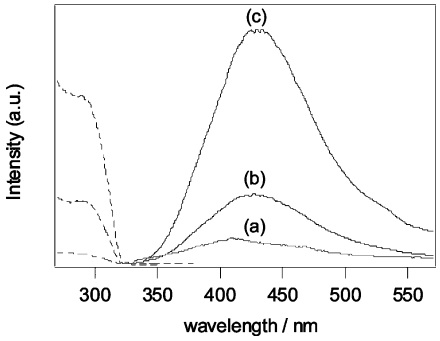

Figure 10. Photoluminescence spectra for β-Ge_3N_4 powders recorded at 77 K. (a) As-synthesized powder. (b, c) Samples treated at 823 K with 20 MPa of NH_3 for (b) 5 h and (c) 24 h (excitation wavelength, 240 nm; emission wavelength, 410 nm).

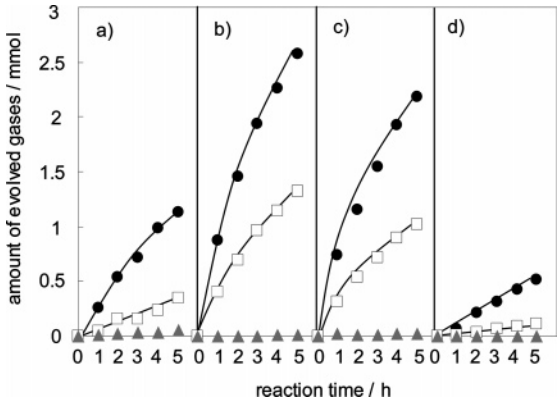

Figure 11. Time courses of evolved gases for β-Ge_3N_4 powders loaded with RuO_2 (1 wt %) as a cocatalyst. (a) As-synthesized powder. (b−d) Samples treated at 823 K with 20 MPa of NH_3 for (b) 5 h, (c) 24 h, and (d) 72 h. Circles denote H_2 evolution, squares denote O_2 evolution, and triangles denote N_2 production.

The photocatalytic activities of samples treated for various periods are shown in Figure 11. Considering the photoluminescence intensity and the extent of absorption decrease in the visible-light region indicated by the UV−visible spectra, it was expected that the sample treated for 24 h would exhibit a higher photocatalytic activity for overall water splitting than the equivalent sample treated for just 5 h. However, all treated samples displayed a consistent 4-fold increase in photocatalytic activity for overall water splitting compared to the as-synthesized powder. The lack of a further increase in photocatalytic activity with prolonged treatment may be attributable to the fact that the photocatalytic activity is dependent on both the bulk state

and the surface state. The decrease in surficial nitrogen concentration (shown in Table 3) that occurs after treatment for 24 h results in a powder with the same photocatalytic activity as for that treated for 5 h. The 72 h-treated sample, however, showed a drop in photocatalytic activity because of the presence of inactive Ge phase.

Conclusions

The photocatalytic activity of β-Ge_3N_4 powder was successfully enhanced by high-pressure ammonia treatment at 823 K for 5−24 h with ammonia pressures of 20 MPa or higher.

The surface and bulk states of the treated samples changed according to the treatment temperature and treatment time. This effect is considered to be related to the stability of β-Ge_3N_4 powder under pressurized ammonia and influenced the photocatalytic activity of the treated catalyst for overall water splitting.

Treatment of β-Ge_3N_4 powder at 823 K for 5 h under 20 MPa ammonia increased the photocatalytic activity of the sample, primarily by reducing the density of defects and impurities in the bulk and surface confirmed by UV−visible DR spectra and XPS analyses. However, treatment at higher or lower temperature resulted in lower photocatalytic activity because of reduction of the β-Ge_3N_4 powder. The optimal treatment conditions also produced a catalyst with greater degree of nitridation compared to the as-synthesized powder. Treatment for longer periods, from 5 to 24 h, resulted in reduction of surface nitrogen. However, extended treatment also increased the photoluminescence intensity and weakened absorption in the visible-light region. This indicates that the density of defects and impurities was further reduced by extended treatment, maintaining the elevated photocatalytic activity despite reduction of surface nitrogen. Treatment for 72 h, however, resulted in a drop in photocatalytic activity because of the presence of the inactive Ge phase.

The optimal conditions for high-pressure ammonia treatment of β-Ge_3N_4 powder as a means of enhancing photocatalytic activity for overall water splitting were thus determined to be a temperature of 823 K, during 5 h, and ammonia pressure of 20 MPa or higher. Treatment of β-Ge_3N_4 powder under these conditions effectively increased the photocatalytic activity by a factor of 4, yielding activities of 1.10 mmol·h^{-1} for H_2 evolution and 0.55 mmol·h^{-1} for O_2 evolution, in comparison with 0.26 mmol·h^{-1} and 0.05 mmol·h^{-1} for the as-synthesized powder. This enhancement can be attributed to reduction of the density of impurities and defects in the powder bulk and surface, which are introduced in the conventional nitridation process.

Acknowledgment. This research was supported by the Solution-Oriented Research for Science and Technology (SORST) program of the Japan Science and Technology Corporation (JST).

References and Notes

(1) Domen, K.; Naito, S.; Soma, M.; Onishi, T.; Tamaru, K. *J. Chem. Soc., Chem. Commun.* **1980**, 543−544.
(2) Lehn, J.; Sauvage, J.; Ziessel, R. *Nouv. J. Chim.* **1980**, *4*, 623−627.
(3) Sato, S.; White, J. M. *Chem. Phys. Lett.* **1980**, *72*, 83−86.
(4) Sayama, K.; Arakawa, H. *J. Photochem. Photobiol. A: Chem.* **1996**, *94*, 67−76.
(5) Domen, K.; Kudo, A.; Shinozaki, A.; Tanaka, A.; Maruya, K.; Onishi, T. *J. Chem. Soc., Chem. Commun.* **1986**, 356−357.
(6) Kudo, A.; Kato, H. *Chem. Phys. Lett.* **2000**, *331*, 373−377.
(7) Ikarashi, K.; Sato, J.; Kobayashi, H.; Saito, N.; Nishiyama, H.; Inoue, Y. *J. Phys. Chem. B* **2002**, *106*, 9048−9053.
(8) Sato, J.; Kobayashi, H.; Ikarashi, K.; Saito, N.; Nishiyama, H.; Inoue, Y. *J. Phys. Chem. B* **2004**, *108*, 4369−4375.
(9) Sato, J.; Saito, N.; Nishiyama, H.; Inoue, Y. *J. Phys. Chem. B* **2001**, *105*, 6061−6063
(10) Frank, S. N.; Bard, A. J. *J. Phys. Chem.* **1977**, *81*, 1484−1488.
(11) Mills, A. *J. Chem. Soc., Chem. Commun.* **1982**, 367−368.
(12) Hitoki, G.; Ishikawa, A.; Takata, T.; Kondo, J. N.; Hara, M.; Domen, K. *Chem. Lett.* **2002**, 736−737.
(13) Hitoki, G.; Takata, T.; Kondo, J. N.; Hara, M.; Domen, K. *Chem. Commun.* **2002**, 1698−1699.
(14) Kasahara, A.; Nukumizu, K.; Hitoki, G.; Takata, T.; Kondo, J. N.; Hara, M.; Kobayashi, H.; Domen, K. *J. Phys. Chem. A* **2002**, *106*, 6750−6753.
(15) Ishikawa, A.; Takata, T.; Kondo, J. N.; Hara, M.; Kobayashi, H.; Domen, K. *J. Am. Chem. Soc.* **2002**, *124*, 13547−13553.
(16) Maeda, K.; Takata, T.; Hara, M.; Saito, N.; Inoue, Y.; Kobayashi, H.; Domen, K. *J. Am. Chem. Soc.* **2005**, *127*, 8286−8287.
(17) Sato, J.; Saito, N.; Yamada, Y.; Maeda, K.; Takata, T.; Kondo, J. N.; Hara, M.; Kobayashi, H.; Domen, K.; Inoue, Y. *J. Am. Chem. Soc.* **2005**, *127*, 4150−4151.
(18) Yoshimura, M.; Suzuki, K.; Somiya, S. *J. Jpn. Soc. Powder Powder Metall.* **1987**, *34*, 78.
(19) Majima, K.; Yagyu, S.; Katsuyama, S.; Nagai, H. *Nippon Kinzoku Gakkaishi* **1993**, *57*(2), 203−208.
(20) Logan, S. R.; Moss, R. L.; Kemball, C. *Trans. Faraday Soc.* **1958**, *54*, 922.
(21) McGill, W. J.; Sebba, F. *J. Catal.* **1963**, *2*, 104−108.
(22) Segal, N.; Sebba, F. *J. Catal.* **1967**, *8*, 105−111.
(23) Aika, K.; Ozaki,A. *J. Catal.* **1969**, *14*, 311−321.
(24) Johnson,W. C. *J. Am. Chem. Soc.* **1930**, 5160−5165.
(25) Deb, S. K.; Dong, J.; Hubert, H.; McMillian, P. F.; Sankey, O. F. *Solid State Commun.* **2000**, *114*, 137.
(26) Leinenweber, K.; O'Keeffe, M.; Somayazulu, M. S.; Hubert, H.; McMillan, P. F.; Wolf, G. H. *Chem. Eur. J.* **1999**, *5*, 3076.
(27) Dong, J.; Sankey, O. F. *Phys. Rev. B* **2000**, *61*, 979.
(28) Ueno, T. *Jpn J. Appl. Phys.* **1983**, *22*, 1349.
(29) Hollinger, G.; Kumurdjian, P.; Mackowski, J. M.; Pertosa, P.; Porte, L.; Duc, T. M. *J. Electron Spectrosc. Relat. Phenom.* **1974**, *5*, 237.
(30) Taylor, J. A.; Lancaster, G. M.; Rabalais, J. W. *J. Electron Spectrosc. Relat. Phenom.* **1978**, *13*, 435.
(31) Ingo, G. M.; Zacchetti, N. *High Temp. Sci.* **1989**, *28*, 137−151.
(32) Bauer, A. A. Private communication, 1965.
(33) Segal, N.; Sebba, F. *J. Catal.* **1967**, *8*, 113.
(34) Mallett, M. W.; Gerds, A. F. *J. Electrochem. Soc.* **1955**, *102*, 292.
(35) Kato, H.; Kudo, A. *J. Phys. Chem. B* **2001**, *105*, 4285.
(36) Anpo, M.; Nakaya, H.; Kodama, S.; Kubokawa, Y.; Domen, K.; Onishi, T. *J. Phys. Chem.* **1986**, *90*, 1633−1636.
(37) Anpo, M.; Yamada, Y.; Kubokawa, Y. *J. Chem. Soc., Chem. Commun.* **1986**, 714−716.